Physiological levels of tumstatin, a fragment of collagen IV α3 chain, are generated by MMP-9 proteolysis and suppress angiogenesis via αVβ3 integrin

Yuki Hamano,[1] Michael Zeisberg,[1] Hikaru Sugimoto,[1] Julie C. Lively,[1,2] Yohei Maeshima,[1] Changqing Yang,[1] Richard O. Hynes,[2] Zena Werb,[3] Akulapalli Sudhakar,[1] and Raghu Kalluri[1,*]

[1]Center for Matrix Biology, Department of Medicine and Gastroenterology, Beth Israel Deaconess Medical Center and Harvard Medical School, Boston, Massachusetts 02215
[2]Department of Biology, Howard Hughes Medical Institute, Center for Cancer Research, Massachusetts Institute of Technology, Cambridge, Massachusetts 02139
[3]Department of Anatomy and Comprehensive Cancer Center, University of California, San Francisco, California 94143
*Correspondence: rkalluri@bidmc.harvard.edu

Summary

We demonstrate a physiological role for tumstatin, a cleavage fragment of the α3 chain of type IV collagen (Col IVα3), which is present in the circulation. Mice with a genetic deletion of Col IVα3 show accelerated tumor growth associated with enhanced pathological angiogenesis, while angiogenesis associated with development and tissue repair are unaffected. Supplementing Col IVα3-deficient mice with recombinant tumstatin to a normal physiological concentration abolishes the increased rate of tumor growth. The suppressive effects of tumstatin require αVβ3 integrin expressed on pathological, but not on physiological, angiogenic blood vessels. Mice deficient in matrix metalloproteinase-9, which cleaves tumstatin efficiently from Col IVα3, have decreased circulating tumstatin and accelerated growth of tumor. These results indicate that MMP-generated fragments of basement membrane collagen can have endogenous function as integrin-mediated suppressors of pathologic angiogenesis and tumor growth.

Introduction

Vascular basement membranes (VBM) are specialized extracellular matrices that provide mechanical support for endothelial cells (Colorado et al., 2000; Madri, 1997; Paulsson, 1992; Timpl, 1996; Yurchenco and O'Rear, 1994) and influence cellular behavior such as differentiation and proliferation (Madri, 1997; Paulsson, 1992; Tsilibary et al., 1990), especially during the sprouting of new capillaries. VBM organization is dependent on the assembly of a type IV collagen network, which is believed to occur via the C-terminal globular non-collagenous (NC1) domain of Col IV (Kuhn, 1995; Madri, 1997; Madri and Pratt, 1986; Timpl, 1996; Tsilibary et al., 1990; Zeisberg et al., 2001; Zhang et al., 1994). Inhibitors of collagen metabolism have antiangiogenic properties, supporting the notion that basement membrane (BM) collagen synthesis and deposition are crucial for blood vessel formation and survival (Maragoudakis et al., 1993, 1995; Tsilibary et al., 1990). Once the endothelium receives signals to proliferate from the tumor microenvironment, it initiates sequential VBM changes that result in exposure of endothelial cells to different isoforms, degradation products, and molecular structures of VBM molecules in a short period of time (Carmeliet and Jain, 2000; Czubayko et al., 1997; Eliceiri et al., 1999; Ferrara, 2000; Folkman, 2001; Folkman and Kalluri, 2003; Hanahan and Weinberg, 2000; Kalluri, 2003; Padera et al., 2002; Stacker et al., 2002).

Our prevailing hypothesis is that such sequential isoform switching and structural changes associated with VBM can provide crucial angiogenic and antiangiogenic stimuli to perpetuate formation of new capillaries (Colorado et al., 2000; Kamphaus et al., 2000; Maeshima et al., 2000a, 2000b, 2001a, 2001b, 2002; Thyboll et al., 2002). There are six distinct gene products, α1-α6 for Col IV (Hudson et al., 1993; Prockop and Kivirikko, 1995). The distribution of the α3 (IV) chain is limited to glomerular BM (GBM), several BM of the cochlea, ocular BM of the anterior lens capsule, Descemet's membrane, ovarian and testicular BM (Frojdman et al., 1998), alveolar capillary BM (Hudson et al., 1993; Kashtan, 1998; Polette et al., 1997), and the VBM of

SIGNIFICANCE

Progression of cancer is dependent on neoangiogenesis. Tumor progression is likely governed by relative levels of pro- and antiangiogenic factors—the "angiogenic balance." Conversion of dormant in situ carcinomas into an invasive malignant phenotype is considered to involve a shift in favor of enhanced angiogenesis potential. Influenced by oncogenes and tumor suppressor genes, disruption of the "angiogenic check point" via increase in angiogenic factors such as VEGF or decrease in the physiological levels of endogenous inhibitors of angiogenesis like thrombospondin-1 and tumstatin could represent an important lethal step in the progression of cancer. Thus, genetic control of the physiological levels of endogenous inhibitors of angiogenesis might constitute a critical last line of defense against conversion of neoplastic events into a malignant phenotype of cancer.

several organs (Derry and Pusey, 1994; Kashtan, 1998), but is absent from epidermal and VBM in the skin (Kashtan, 1998).

During BM synthesis, turnover fragments are generated which are liberated into the circulation, raising the question as to whether they have any physiological function (Hogemann et al., 1984; Ortega and Werb, 2002; Standker et al., 1997). The bioactive NC1 domain of Col IVα3, called tumstatin, acts as an angiogenesis inhibitor, inhibiting the proliferation of capillary endothelial cells and blood vessel formation in vitro and in vivo (Maeshima et al., 2000a, 2000b, 2001a, 2001b; Petitclerc et al., 2000). Deletion mutagenesis experiments have narrowed the biological activity to a 25 amino acid stretch in the middle of the molecule (Maeshima et al., 2001b). Tumstatin binds to αVβ3 integrin via a mechanism independent of the RGD-containing amino acid sequence (Maeshima et al., 2000a). However, since previous studies relied on exogenous addition of tumstatin (or fragments of other basement membrane collagens), this raises the question of whether such fragments have an endogenous physiological function. Here we provide genetic evidence supporting a role for tumstatin as an endogenous suppressor of pathological angiogenesis and tumor growth.

Results

Mice with deletion of collagen IV α3 (tumstatin precursor) exhibit normal pregnancy, development, and wound healing, but accelerated pathologic angiogenesis and tumor growth

Angiogenesis plays an important role during pregnancy and embryonic development. Tumstatin, which has a circulating physiological concentration of about 336 $\pm$ 28 ng/ml in normal mice, was absent in mice deficient in α3 chain of Col IV, the precursor for tumstatin (Figures 1A and 1B), without altering the litter size, pregnancy, or development (Figures 1C and 1D). In the present study, we refer to the Col IVα3-deficient mice (Andrews et al., 2002; Cosgrove et al., 1996; Miner and Sanes, 1996) as also tumstatin deficient. After week 20, these mice on C57BL/6 background develop kidney dysfunction associated with GBM abnormalities and inflammation and die at around week 40 due to renal failure resulting from the absence of Col IVα3 in the GBM (Andrews et al., 2002; data not shown).

Next, we evaluated tumor-associated pathological angiogenesis in Col IVα3/tumstatin-deficient mice on a C57BL/6 background. Tumors from Lewis lung carcinoma (LLC) cells (10^6) placed on the backs of mice appeared at about 7 days and grew at the same rate in wild-type and Col IVα3/tumstatin-deficient mice until they reached about 500 mm^3 of tumor volume (Figure 2A). Consistently, from this size, the tumors on Col IVα3/tumstatin-deficient mice grew at a faster rate and, by day 26, the tumors on the Col IVα3/tumstatin-deficient mice were more than twice the size of wild-type tumors (Figure 2A). Administration of 300 ng of recombinant human tumstatin, which has a half-life of about 20 hr in mice (data not shown), daily to the Col IVα3/tumstatin-deficient mice with 500 mm^3 LLC tumors, decreased tumor growth to wild-type levels (Figure 2A). These experiments demonstrate that restoration of physiological levels of tumstatin in Col IVα3/tumstatin-deficient mice suppresses the accelerated growth of tumors (Figure 2A). Similar results were obtained with syngeneic B16F10 melanoma and T241 fibrosarcoma tumors (O'Reilly et al., 1997) in Col IVα3/tumstatin-deficient mice (data not shown).

To determine if altered vascularity was the underlying mechanism of the increased tumor growth, we analyzed a second type of pathological angiogenesis in the growth factor-supplemented Matrigel plug assay. We observed increased angiogenesis in the Col IVα3/tumstatin-deficient mice, as compared to the wild-type mice (Figure 2B). Col IVα3/tumstatin-deficient mice demonstrating increased rate of tumor growth had increased numbers of CD31-positive blood vessels (Figure 2C). Recent studies have suggested that increases in the circulating vascular endothelial growth factor receptor 2 (VEGFR2)-positive endothelial cells correlate directly with increase in tumor angiogenesis and can serve as in vivo indicators of tumor angiogenesis (Heissig et al., 2002; Lyden et al., 2001; Monestiroli et al., 2001). Col IVα3/tumstatin-deficient mice had increased circulating VEGFR2-positive endothelial cells (Figure 2D).

If the regulation of angiogenesis relies on the presence of circulating tumstatin, then exogenous addition of tumstatin to physiological levels in the null mice should decrease the number of blood vessels and circulating endothelial cells to the wild-type baseline levels. Indeed, we observed suppression of tumor angiogenesis to wild-type levels (Figures 2C and 2D), indicating that the lack of tumstatin domain alone is responsible for the accelerated tumor growth in the Col IVα3-deficient mice.

By contrast, physiological angiogenesis associated with tissue repair was unaffected in the Col IVα3/tumstatin-deficient mice. Closure/repair in skin wounds progressed at the same rate in the wild-type and the null mice (Figure 3A) and showed insignificant differences in histology and CD31-positive blood vessels (Figures 3A and 3B). Similarly, regeneration of liver after partial hepatectomy was similar in the wild-type and null mice. The rates of regeneration assessed by the proliferation index of the liver, as determined by BrdU staining (Figure 3C), and angiogenesis, assessed by the number of von Willebrand Factor (vWF)-positive blood vessels (Figure 3D), were similar in the wild-type and null mice.

Antiangiogenic activity of tumstatin requires αVβ3 integrin

Tumstatin binds to αVβ3 integrin in a vitronectin/RGD sequence-independent manner (Maeshima et al., 2000a). If the antiangiogenic action of tumstatin is mediated through this receptor, then cells and mice lacking αVβ3 integrin should not respond to it. Tumstatin or active derivative T7 peptide (Maeshima et al., 2001b) at 1 μM, which has been shown previously to achieve maximum inhibition of endothelial cell proliferation (Maeshima et al., 2000b), significantly inhibited proliferation of wild-type mouse lung endothelial cells (MLEC) in response to growth factor stimulation, while proliferation of β3 integrin null MLEC was unaffected (Figure 4A). By contrast, mouse endostatin (the NC1 domain of α1 chain of collagen XVIII) was equally effective in inhibiting the proliferation of both wild-type and β3 integrin null MLEC (Figure 4A).

Neovascularization of growth factor-supplemented Matrigel plugs in mice is associated with significant expression of β3 integrin (Figure 4B). We next evaluated the antiangiogenic activity of tumstatin in vivo in the Matrigel plug assay system in wild-type and β3 integrin-deficient mice on the C57BL/6 background. Both tumstatin and endostatin significantly inhibited VEGF-induced neovascularization of the plugs in the wild-type mice (Figure 4C). However, while endostatin significantly inhibited blood vessels in the Matrigel plugs implanted in the β3

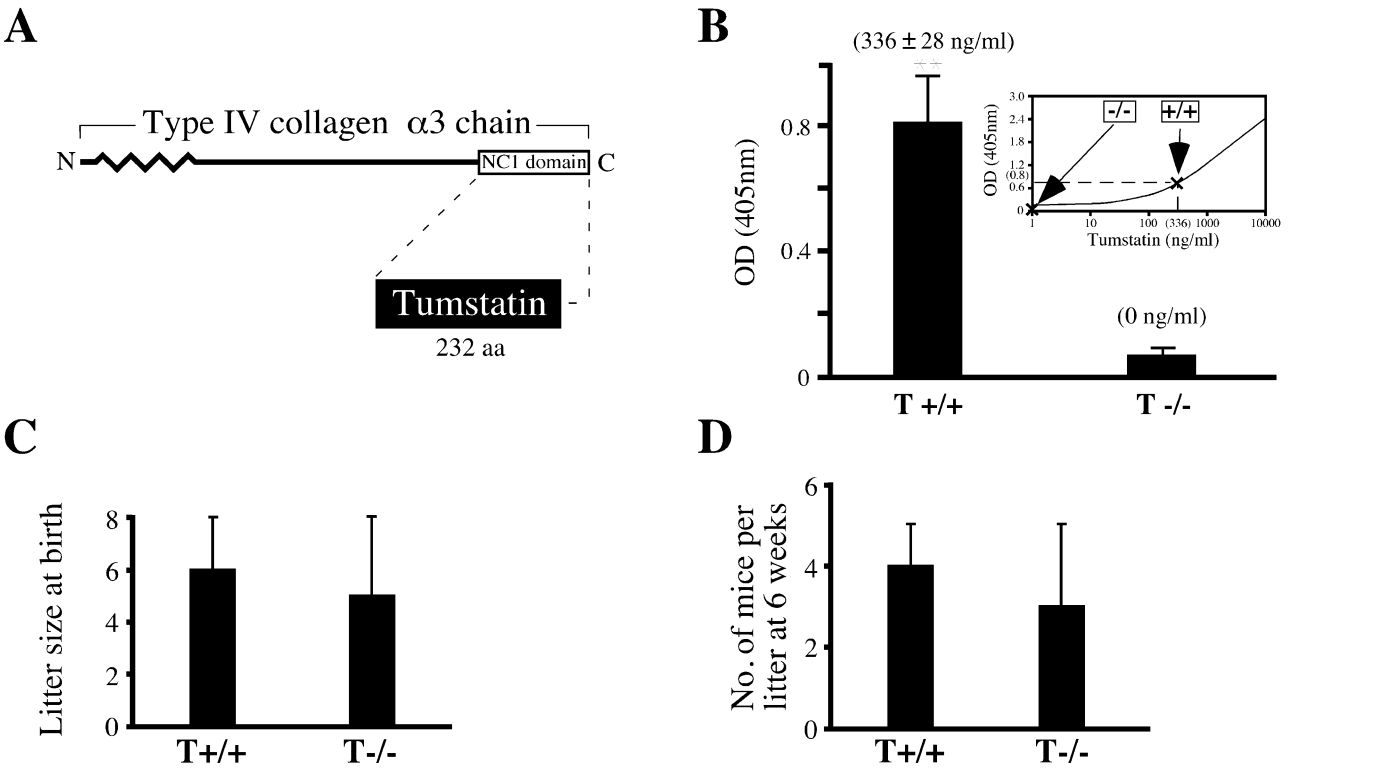

Figure 1. Tumstatin and Col IVα3/tumstatin$^{-/-}$ mice

A: Schematic illustration of the type IV collagen α3 chain and tumstatin. Tumstatin (solid shading) is indicated in relation to type IV collagen α3 chain.
B: Circulating levels of tumstatin in mouse blood. The plasma from ten wild-type (T$^{+/+}$) and ten Col IVα3/tumstatin$^{-/-}$ (T$^{-/-}$) mice was examined using direct ELISA with anti-tumstatin antibody. Standard curve was calculated using recombinant tumstatin protein and anti-tumstatin antibody. ** indicates $p < 0.01$; compared to T$^{-/-}$. The results are shown as the mean ± SEM.
C and **D:** Litter size and development of Col IVα3/tumstatin$^{-/-}$ mice. To evaluate litter size at birth, an average number of eight separate litters delivered by T$^{+/+}$ and T$^{-/-}$ parents was counted. In order to evaluate early development of pups, a 6 week survival rate for eight separate litters from both groups was calculated. The results are shown as the mean ± SD.

integrin-deficient mice, tumstatin had an insignificant effect (Figure 4C). These data suggest that tumstatin action in vivo is likely mediated by αVβ3 integrins.

Tumstatin functions as an inhibitor of tumor-associated pathological angiogenesis, while having no effect on physiological angiogenesis due to differential expression of β3 integrin

How can tumstatin function as an inhibitor of tumor-associated pathological angiogenesis, while having no effect on physiological angiogenesis associated with repair and regeneration of skin and liver? Our experiments suggest that tumstatin depends on αVβ3 integrin for inhibition of tumor-associated pathological angiogenesis. We detected αVβ3 integrin on about 40% of the blood vessels and small capillaries in proliferating tumors; however, we did not detect it in the blood vessels of healing skin wounds or regenerating livers (Figure 5A). In contrast, β1 integrin was detected on all blood vessels and capillaries associated with tumor growth, healing wounds, and regenerating skin liver (Figure 5B). Such differences in αVβ3 integrin levels may explain the lack of tumstatin effect on repair and regeneration, while targeting tumor vasculature (Figure 3).

Why do tumors grow faster in the Col IVα3/tumstatin-deficient mice only after they reach a size of 500 mm^3? To address this issue, we assessed the vascular expression of β1 and β3 integrin in tumors starting from a size of 100 mm^3 to 5000 mm^3. Interestingly, our results indicate that while β1 was expressed in about 80% of the blood vessels even in tumors as small as 100 mm^3, β3 integrin was expressed in only about 8% of capillaries at this stage (Figure 6). The β3 expression increased to about 40% of the blood vessels by the time the tumors reached 500 mm^3 and remained at that level, no matter how large the tumor (Figure 6). Expression of β1 integrin at this stage continued to be detected in 80% of the blood vessels. Since significant β3 integrin expression on the vasculature was seen only beginning at the size of 500 mm^3 and tumstatin does not induce negative regulation when the tumors are smaller than 500 mm^3 (Figures 2, 4, 5 and 6), the vascular expression pattern of β3 integrin provides a possible explanation for the lack of tumor growth difference between the wild-type and Col IVα3/tumstatin-deficient mice until the tumors reach the size of 500 mm^3.

Degradation of basement membrane type IV collagen by MMP-9 generates tumstatin

How is tumstatin generated from BM collagen? BM-degrading MMPs that degrade Col IV could potentially liberate fragments such as NC1 domains of Col IV (Kalluri, 2003; McCawley and

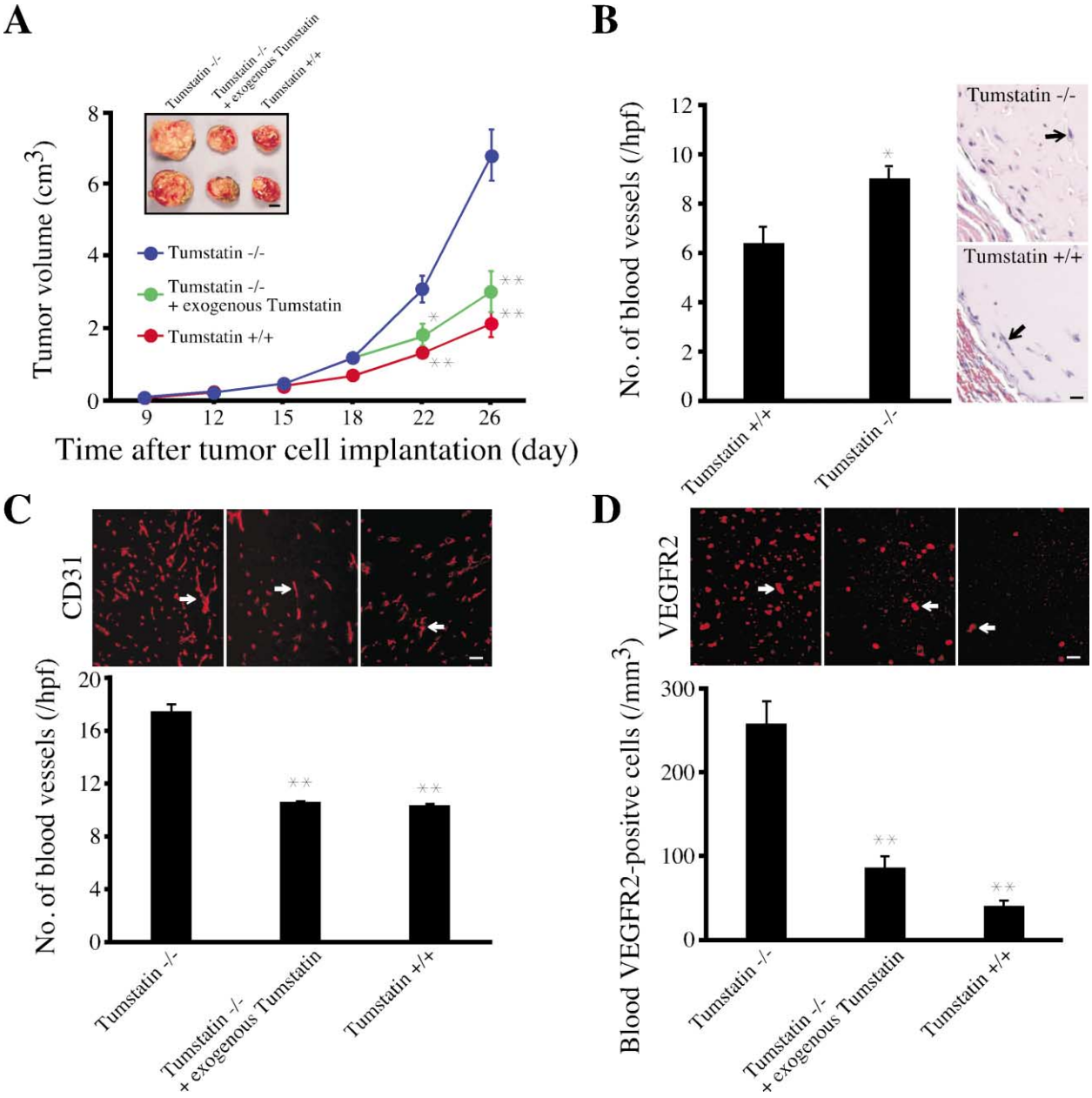

Figure 2. Tumor burden studies in Col IVα3/tumstatin-deficient mice

A: LLC tumor growth in Col IVα3/tumstatin$^{-/-}$ mice. Twelve age- and sex-matched Col IVα3/tumstatin$^{-/-}$ mice and six wild-type mice were used in this experiment. Recombinant tumstatin protein was intravenously injected into seven Col IVα3/tumstatin$^{-/-}$ mice daily (300 ng) for 8 days starting at day 18 in sterile PBS, while only PBS was injected into the other five Col IVα3/tumstatin$^{-/-}$ mice. Data are representative of four such independent experiments. The results are shown as the mean ± SEM. ** indicates $p < 0.01$; * indicates $p < 0.05$; compared to Col IVα3/tumstatin$^{-/-}$ mice without injection. Scale bar: 1 cm.

B: Matrigel plug assay in Col IVα3/tumstatin$^{-/-}$ mice. Sections of each Matrigel plug were stained with HE and the numbers of blood vessels (arrow) in ten fields at 200× magnification were counted. Each column represents the mean ± SEM of six mice in each group. * indicates $p < 0.05$; compared to Col IVα3/tumstatin$^{+/+}$ mice. Scale bar: 50 μm.

C: Blood vessel quantification in LLC tumors. Frozen sections (4 μm) from tumor tissue were stained with anti-CD31 antibody, and the number of CD31-positive blood vessels (arrow) was counted. The results are shown as the mean ± SEM. ** indicates $p < 0.01$; compared to Col IVα3/tumstatin$^{-/-}$ mice. Scale bar: 50 μm.

D: VEGF receptor 2 (VEGFR2)-positive circulating endothelial cells in mice. The blood cells from peripheral blood attached to the slide were stained with anti-VEGFR2 antibody, and the number of positive cells (arrow) was counted. The results are shown as the mean ± SEM. ** indicates $p < 0.01$; compared to Col IVα3/tumstatin$^{-/-}$ mice. Scale bar: 50 μm.

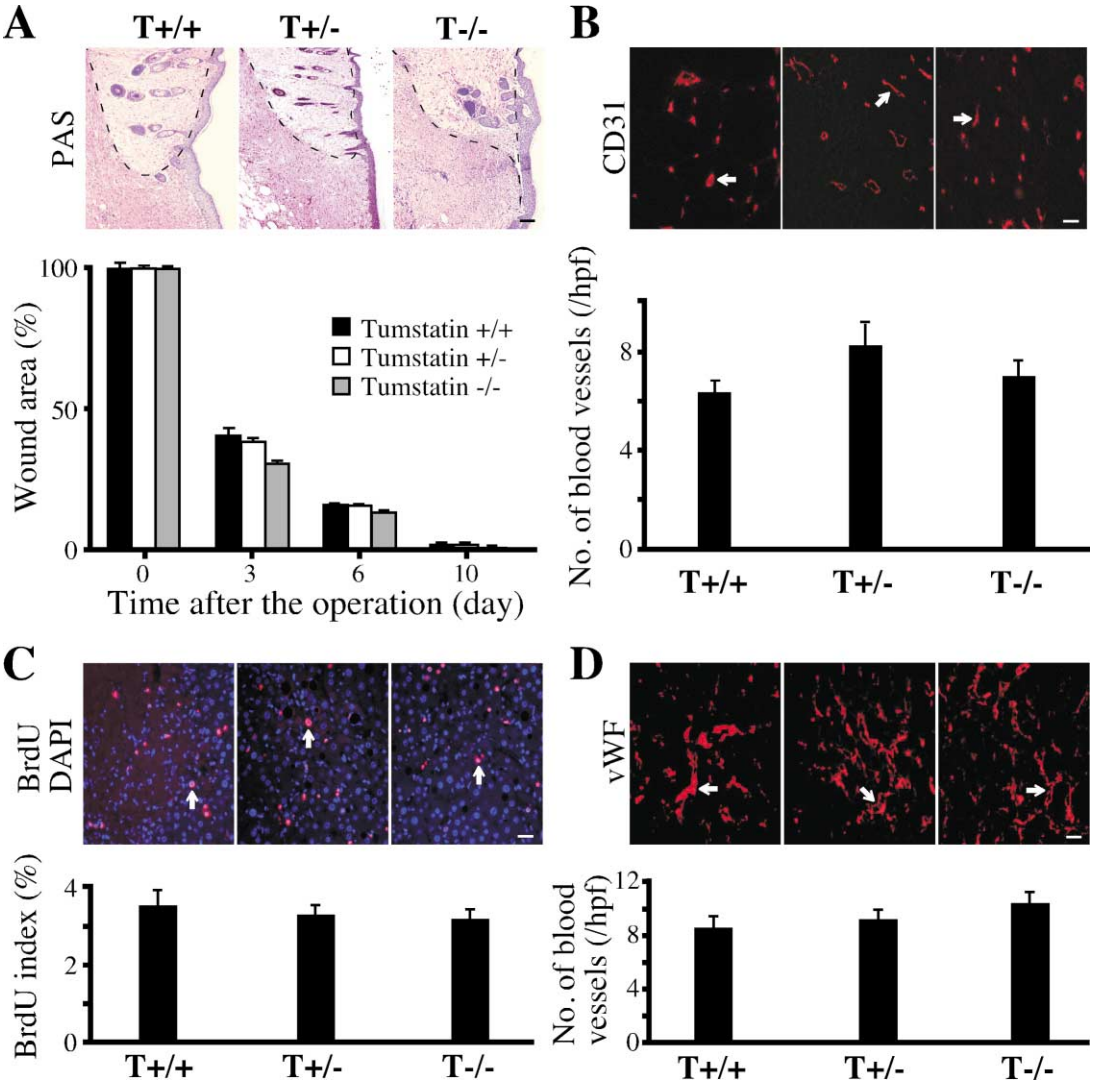

Figure 3. Repair-associated angiogenesis in Col IVα3/tumstatin-deficient mice

A: Skin wound healing in Col IVα3/tumstatin$^{-/-}$ mice. One centimeter diameter skin wounds were induced in five wild-type ($T^{+/+}$), five Col IVα3/tumstatin$^{+/-}$ ($T^{+/-}$), and five Col IVα3/tumstatin$^{-/-}$ ($T^{-/-}$) mice. The areas were measured periodically as indicated and the ratio in relation to the original wound size at day 0 was calculated at each time point. There was insignificant difference in the wound healing among the groups at all time points. The results are shown as the mean ± SEM. The PAS-stained wound areas at day 10 are shown here. Scale bar: 50 μm.

B: Quantification of blood vessels in the skin. Frozen sections (4 μm) were stained with the anti-CD31 antibody and the numbers of CD31-positive blood vessels (arrow) were counted. The results are shown as the mean ± SEM. Scale bar: 50 μm.

C and **D:** Liver regeneration in Col IVα3/tumstatin$^{-/-}$ mice. Seventy percent of the liver was removed in $T^{+/+}$, $T^{+/-}$, and $T^{-/-}$ mice with five mice per group. The proliferating hepatic cells were double-stained with BrdU and DAPI (arrow). Frozen sections (4 μm) from liver tissue were stained with anti-von Willebrand Factor (vWF) antibody to evaluate blood vessels (arrow). The results are shown as the mean ± SEM. Scale bar: 50 μm.

Matrisian, 2001). We found that active MMP-9 was most effective in liberating C-terminal NC1 globular domains in dimeric and monomeric forms, detected in the supernatant by polyclonal tumstatin antibody, from the GBM which is rich in the Col IVα3 chain (Frojdman et al., 1998; Gunwar et al., 1991; Kalluri and Cosgrove, 2000) (Figures 7A and 7B). Three other BM-degrading proteinases, MMP-2, MMP-3, and MMP-13, also released tumstatin, but were significantly less efficient (data not shown). MMP-9 is significantly less efficient in liberating arresten and canstatin from BMs, when compared to tumstatin (data not shown).

Mice deficient in MMP-9 had significantly decreased circulating blood concentrations of tumstatin; 141 ± 21 ng/ml, compared with 350 ± 24 ng/ml in the wild-type mice ($p < 0.01$). These results suggest that normal physiological turnover of BM by MMPs, especially MMP-9, contributes to the circulating levels of tumstatin.

Restoration of tumstatin levels inhibits the increased tumor growth rate in MMP-9-deficient mice

What circulating levels of tumstatin are required to inhibit tumor growth? The growth of LLC tumors implanted into wild-type mice and MMP-9-deficient mice on a C57BL/6 background was similar until the tumors reached 500 mm^3, but after that, the tumors on MMP-9-deficient mice exhibited accelerated growth

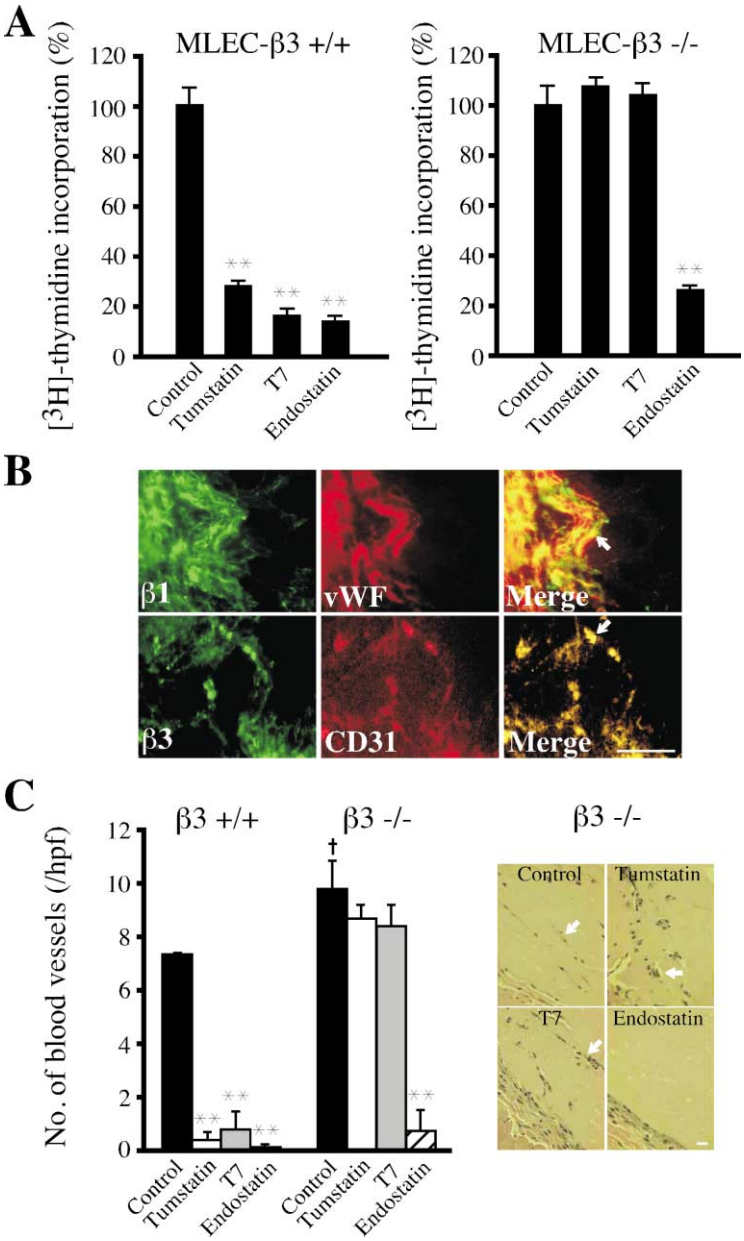

Figure 4. Tumstatin activity in β3 integrin-deficient mice

A: Proliferation assay in β3 integrin$^{-/-}$ endothelial cells. MLEC were isolated from wild-type (β3$^{+/+}$) and β3 integrin$^{-/-}$ (β3$^{-/-}$) mice as previously described (Maeshima et al., 2002). Proliferation was assessed by [^{3}H]-thymidine incorporation. All groups represent triplicate analyses. The results are shown as the mean ± SEM. ** indicates $p < 0.01$; compared to control cells.

B: Expression of β1 and β3 integrins in blood vessels of Matrigel plug. β1 and β3 integrin-positive blood vessels are indicated with arrows. Scale bar: 50 μm.

C: Matrigel plug assay in β3 integrin$^{-/-}$ mice. Sections of each Matrigel plug were stained with HE and the number of blood vessels (arrow) was counted. Each column represents the mean ± SEM of 2–4 mice in each group. Data are representative of two independent Matrigel plug experiments. ** indicates $p < 0.01$; compared to each control groups. † indicates $p < 0.05$; compared to the control group in β3 integrin$^{+/+}$ mice. Scale bar: 50 μm.

(Figure 8A). Injection of 200 ng of recombinant human tumstatin intravenously daily for 14 days into MMP-9-deficient mice with established tumors raised the concentration of tumstatin to the normal levels of about 342 ± 13 ng/ml (data not shown) and resulted in a retarded rate of growth to match the wild-type tumor growth (Figure 8A, inset). This deceleration of tumor growth was accompanied by decreased numbers of CD31-positive blood vessels and VEGFR2-positive circulating endothelial cells (Figures 8B and 8C). Collectively, these results suggest that the increase in LLC tumor growth in MMP-9-deficient mice was due to decreased physiological levels of tumstatin.

Discussion

Basement collagens in their native molecular structure form a scaffold for cell homeostasis. In this study, we have demonstrated that tumstatin, a BM Col IVα3 chain-derived NC1 domain, can be detected in the circulation of normal mice and functions as an endogenous regulator of pathologic angiogenesis and that the activity of tumstatin is dependent on αVβ3 integrin and the ECM-degrading enzyme, MMP-9.

The Col IVα3 chain is localized to many VBM and is most abundant in the GBM of the kidney and the BM of the testis (Frojdman et al., 1998; Hudson et al., 1993; Kahsai et al., 1997). It is likely that physiological turnover of GBM and other BM mediated by ECM-degrading MMPs contributes to the circulating physiological levels of tumstatin. Col IVα3 chain-deficient mice do not have circulating tumstatin, and syngeneic LLC tumors larger than 500 mm^3 on these mice grew at more than twice the rate of tumors on wild-type mice. This difference in growth could be restored to wild-type levels when the null mice were provided with physiological concentrations of tumstatin in

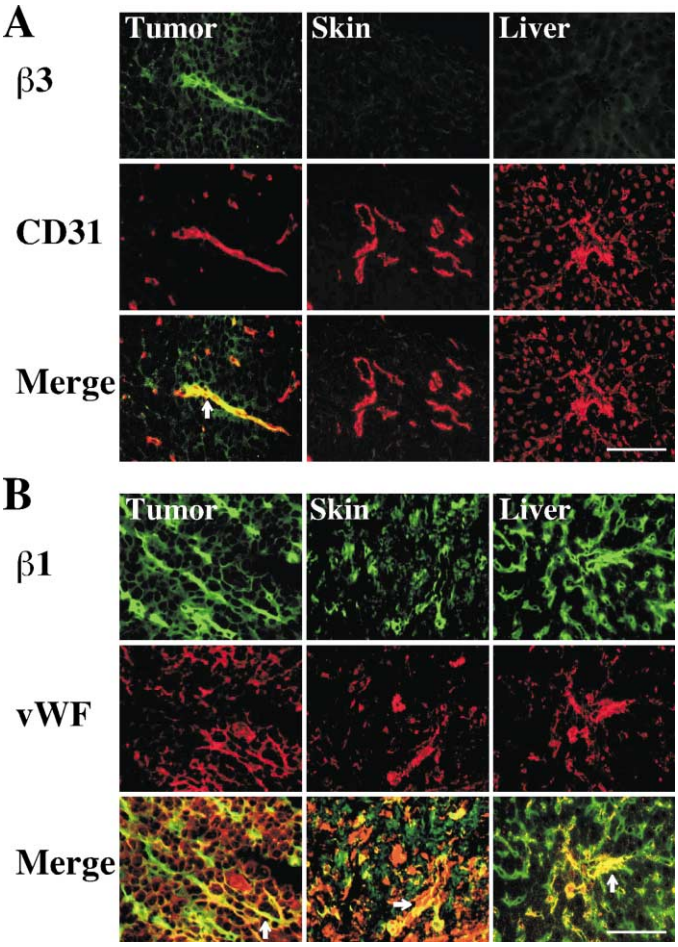

Figure 5. Expression of β3 and β1 integrins in tumors, healing skin wound, and regenerating livers

A: Immunohistochemical staining with anti-β3 integrin (β3) antibody and CD31 or vWF was performed to assess localization of β3 integrin in blood vessels. Anti-CD31 antibody was used for the tumor and skin tissues and anti-vWF antibody was used for the liver tissue. β3 integrin-positive blood vessels (merge) are indicated with arrows. Scale bar: 50 μm.
B: β1 integrin expression in the tumor, skin wound, and regenerating liver tissues. β1 integrin-positive blood vessels (merge) are shown here. β1 integrin-positive vessels are indicated with arrows. Scale bar: 50 μm.

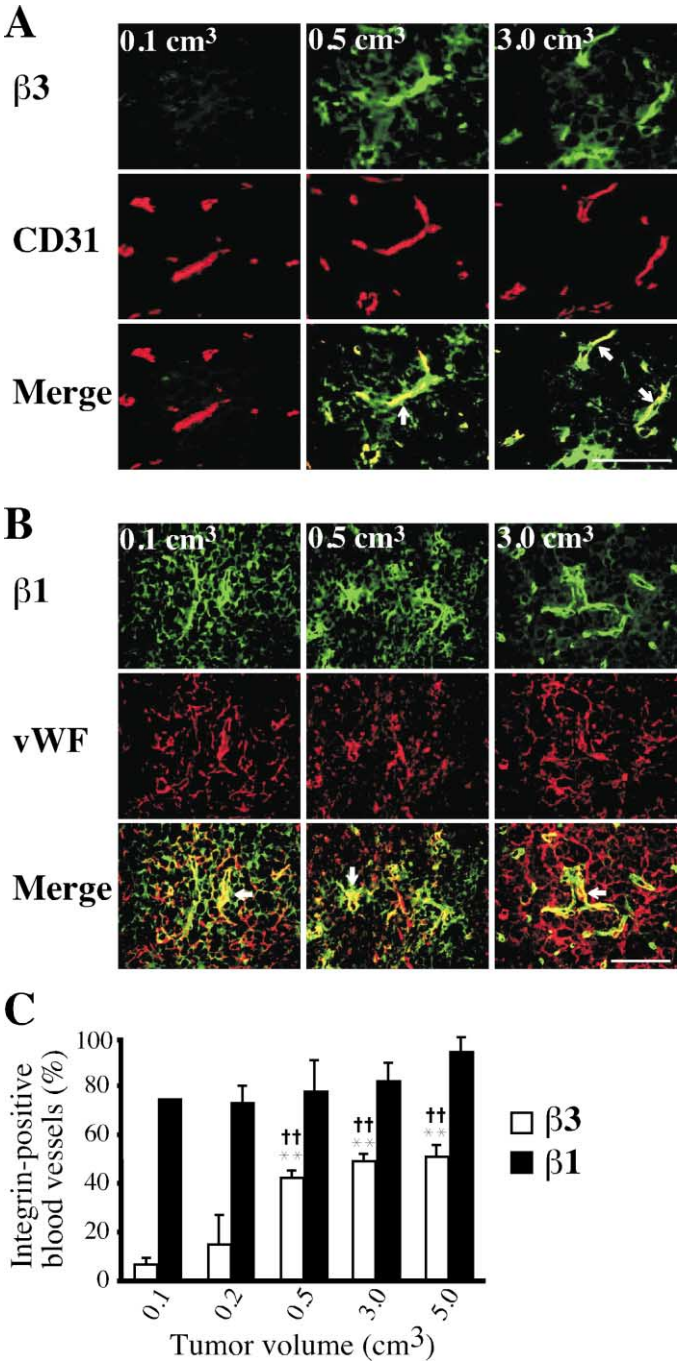

Figure 6. Expression of β3 and β1 integrins in tumors of various sizes

A: Immunohistochemical staining with anti-β3 integrin (β3) antibody and CD31 was performed to assess localization of β3 integrin in the tumor blood vessels with volumes of 0.1, 0.5 and 3.0 cm^3 in wild-type mice. β3 integrin-positive blood vessels (merge) are indicated with arrows. Scale bar: 50 μm.
B: β1 integrin expression in tumors with volumes of 0.1, 0.5, and 3.0 cm^3. β1 integrin-positive vessels (merge) are indicated with arrows. Scale bar: 50 μm.
C: Quantification of β1/β3 integrin-positive blood vessels in the tumor. The ratio of β3 integrin-positive blood vessels to CD31-positive vessels (open bar) was calculated in the tumors with various volumes. As a control, the ratio of β1 integrin-positive blood vessels to vWF-positive vessels (closed bar) was also calculated. ** indicates $p < 0.01$; compared to β3 integrin-positive blood vessels in 0.1 cm^3 of tumor. †† indicates $p<0.01$; compared to β3 integrin-positive blood vessels in 0.2 cm^3 of tumor.

recombinant form. These results suggest that the acceleration of tumor growth in the null mice is not due to the absence of α3 (IV) chain, but is likely due the lack of the tumstatin domain. Our study distinguishes the physiological role of tumstatin from its potential pharmacological applications. Providing tumstatin (300 ng/day, i.v.) to the null mice slowed the tumor growth to the wild-type level, but did not cause regression or inhibition of tumor growth. The pharmacological doses needed to achieve inhibition of LLC tumor growth are much higher, in the range of 5–15 μg/day, i.v. (data not shown). Further studies are required to understand what mechanisms drive the switch between the physiological and pharmacological functions of tumstatin.

An interesting insight into the physiological role of tumstatin in the suppression of tumstatin can be made from the observation that, until the tumors reach 500 mm^3, the difference in tumor growth between the wild-type mice and Col IVα3/tumstatin-

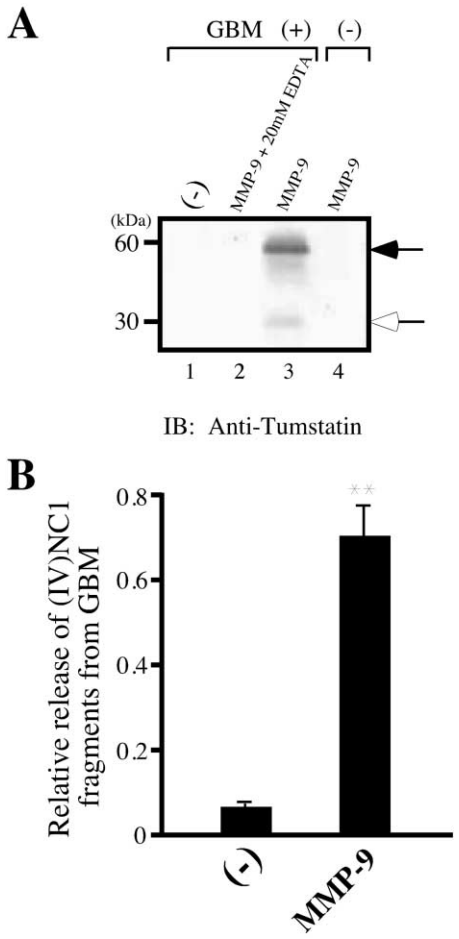

Figure 7. Degradation of basement membrane preparation by active MMP-9

A: Western blot of BM degraded by MMP-9. MMP-9 enzyme was added to GBM at a 1:100; enzyme:substrate ratio, and the generation of tumstatin was detected by SDS-PAGE and immunoblotting using anti-tumstatin antibody. To establish MMP specificity in generation of tumstatin, 20 mM EDTA was added to the MMP/GBM mixture to inactivate MMP. The expected dimer (black arrow) and monomer (white arrow) of tumstatin are indicated. Monomers and dimers of type IV collagen NC1 domain have been previously described (Kalluri et al., 1997b).

B: Quantification of tumstatin production by MMP-9 by ELISA. MMP-9 enzyme was added to 1 mg of GBM, and the production of soluble tumstatin in the supernatant was analyzed by ELISA using anti-tumstatin antibody. The results are shown as the mean ± SD. ** indicates $p < 0.01$; compared to the control group without enzyme.

deficient mice is insignificant. Our results suggest that lack of significant vascular expression of β3 integrin until the tumors reach 500 mm^3 is a likely explanation for the insignificant difference in the growth of tumor in the absence of tumstatin before tumors reach 500 mm^3. Alternatively, it is possible that during the early growth phase of the tumors, absence of tumstatin can be compensated by other inhibitors of angiogenesis, such as thrombospondin-1, angiostatin, and endostatin (Hawighorst et al., 2001; O'Reilly et al., 1994, 1997; Rodriguez-Manzaneque et al., 2001; Volpert et al., 2002). But once the tumor reaches a critical size and β3 integrin expression increases significantly, the entire antiangiogenic arsenal including tumstatin is required for the control of tumor growth.

We previously implicated αVβ3 integrin as a putative receptor for tumstatin and the binding between them (Maeshima et al., 2000a, 2001a, 2001b, 2002) is independent of RGD sequence, vitronectin, and fibronectin binding. In the present study, we used genetic experiments with β3-deficient mice to demonstrate that αVβ3 integrin mediates tumstatin action. Tumors also grow faster in β3-deficient mice than in wild-type mice (Reynolds et al., 2002). Collectively, these observations strongly suggest a role for αVβ3 integrin as a negative regulator of angiogenesis (Hynes, 2002a; Hynes et al., 2002b; Kalluri, 2002; Maeshima et al., 2001a).

Our experiments suggest that tumor angiogenesis, but not angiogenesis associated with the repair of skin wound and regeneration of liver, is associated with robust expression of β3 integrins, including αVβ3 integrin. This is likely the explanation for the lack of difference on the skin wound repair and liver regeneration in the Col IVα3/tumstatin-deficient mice and also in pharmacological studies with recombinant human tumstatin (data not shown). Both Col IVα3/tumstatin-deficient mice and β3 integrin-deficient mice on a C57BL/6 background do not exhibit developmental angiogenesis defects (Andrews et al., 2002; Cosgrove et al., 1996; Hodivala-Dilke et al., 1999), suggesting that β3 integrin and tumstatin may not be essential for the regulation of developmental angiogenesis.

MMP-9 has been implicated in the degradation of type IV collagen present in the BM (Egeblad and Werb, 2002; McCawley and Matrisian, 2001), and fragments of Col IV and laminin have been detected in the serum of normal individuals and cancer patients (Gabrielli et al., 1988; Yudoh et al., 1994). Tumstatin is a proteolytic product that has to be liberated from the parent Col IVα3 chain. MMP-9 was the most effective enzyme in the generation of tumstatin domain from BM and type IV collagen preparations from the human kidney, testis, and placenta and amnion. We demonstrated that mice deficient in MMP-9 have lower circulating levels of tumstatin, and that this results in increased tumor growth. The accelerated tumor growth can be restored to wild-type levels by supplementing the null mice with the missing physiological concentration of tumstatin. Moreover, Col IV is elevated in the tumor tissue and also in the GBM of MMP-9-deficient mice (data not shown). Such increased accumulation is likely due to reduced Col IV turnover in the mice. These results provide further evidence for the endogenous tumor-suppressive action of tumstatin.

However, MMP-9 has also been implicated as a positive regulator of the angiogenic switch, which leads to early stage tumor differences resulting in lower tumor size and volume (Bergers et al., 2000). But, in the same mice at a later stage, the tumor size and volume catch up with the wild-type levels, suggesting an acceleration of tumor growth in the absence of MMP-9, as observed in the present study (personal communication, G. Bergers and D. Hanahan). In this regard, Pozzi et al. recently demonstrated that pharmacological inhibition of MMP-9 in mice results in acceleration of tumor growth, further supporting our observation (Pozzi et al., 2000, 2002). Thus, MMP-9 has opposing actions on neoplasia at different stages of tumor progression. While it may mediate the angiogenic switch leading to the initial burst of tumor growth, it also restrains tumor development by generating endogenous inhibitors of angiogenesis such as tumstatin. After the angiogenic switch has been

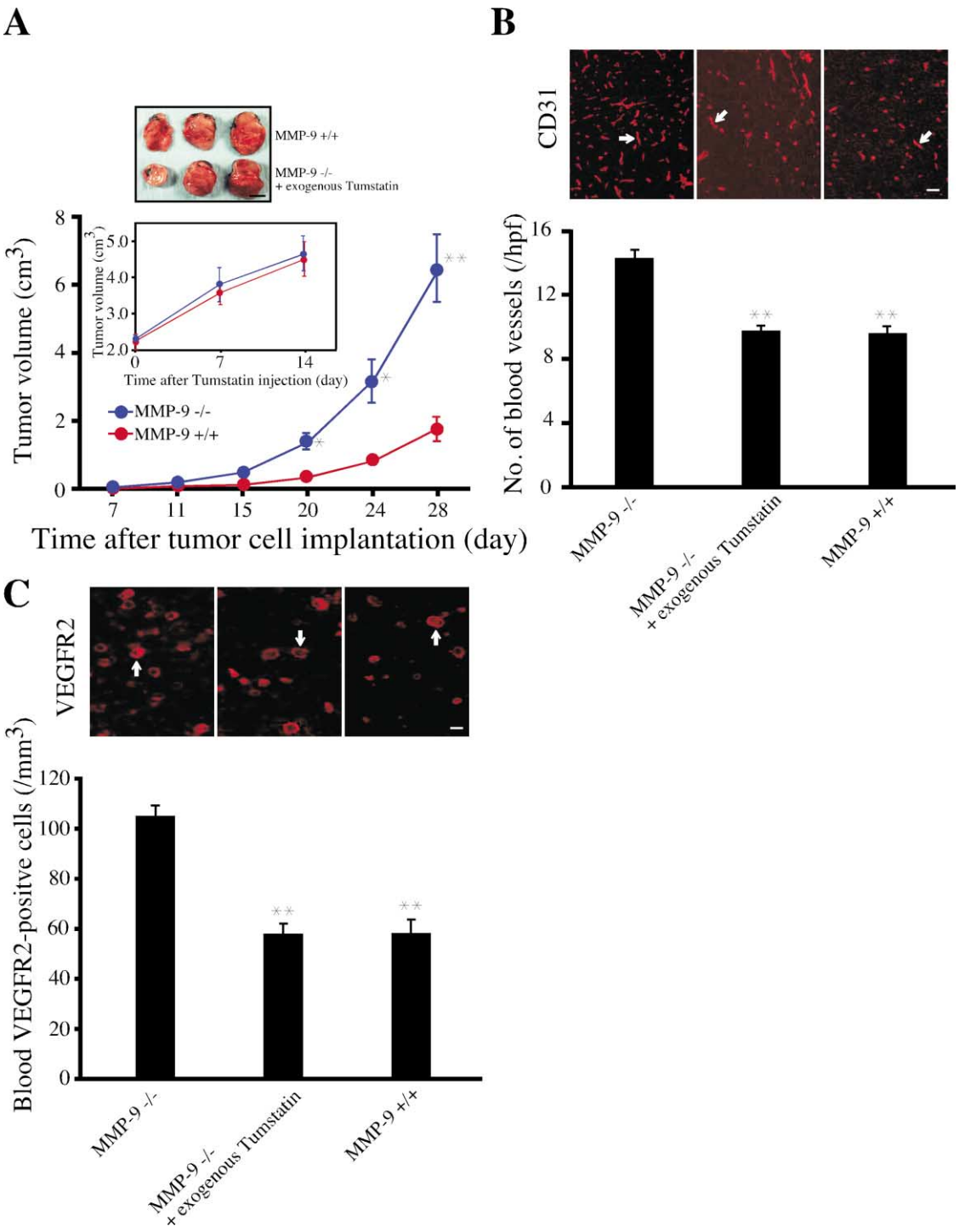

Figure 8. Enhanced tumor growth in MMP-9-deficient mice

A: LLC tumor growth in MMP-9$^{-/-}$ mice. Eight age- and sex-matched MMP-9$^{-/-}$ mice and ten wild-type mice were used for this experiment. While at the very early stages (between 50 mm^3 and 100 mm^3), MMP-9$^{-/-}$ tumors grew slightly slower; after that (especially >500 mm^3), they grew at a much faster rate compared to wild-type tumors. Circulating levels of tumstatin were 350 ng/ml in wild-type mice compared to 141 ng/ml in the MMP-9$^{-/-}$ mice. When the tumor volume reached 2.0 cm^3, tumstatin was intravenously injected into four MMP-9$^{-/-}$ mice (200 ng/day) for 14 days. Their tumor growth was compared to wild-type tumors starting at a size of 2.0 cm^3. For these experiments, the tumors in the wild-type and MMP-9$^{-/-}$ mice were grown until the both sets of tumors reached 2.0 cm^3 (the wild-type tumors take 28 days to reach this size, while tumors in MMP-9$^{-/-}$ mice take 21 days to reach this size). The accelerated tumor growth in MMP-9$^{-/-}$ mice was suppressed by exogenous tumstatin, when compared with wild-type mice. The results are shown as the mean ± SEM. ** indicates $p < 0.01$; * indicates $p < 0.05$; compared to wild-type mice. Scale bar: 1 cm.

B: Blood vessel quantification in LLC tumors. Frozen sections (4 μm) from tumor tissue were stained with anti-CD31 antibody and the number of CD31-positive blood vessels (arrow) counted. The results are shown as the mean ± SEM. ** indicates $p < 0.01$; compared to MMP-9$^{-/-}$ mice. Scale bar: 50 μm.

C: VEGFR2-positive circulating endothelial cells in mice. Cells from peripheral blood were stained with VEGFR2 antibody and the numbers of positive cells (arrow) were counted. The results are shown as the mean ± SEM. ** indicates $p < 0.01$; compared to MMP-9$^{-/-}$ mice. Scale bar: 50 μm.

achieved by MMP-9, the degradation products resulting from digestion of BM by the increased amount of MMP-9 negatively influence the growth of tumors. Therefore, the two opposite properties of MMP-9 are integral to the overall progression of tumor growth. In this regard, recent clinical trial failures with MMP inhibitors could be explained by our data, although early intervention of tumor growth by MMP inhibitors is still potentially feasible (Bramhall et al., 2002).

What roles do the other physiological angiogenesis inhibitors play? Interestingly, endostatin (type XVIII collagen)-deficient mice have altered retinal vascular development, but do not exhibit accelerated tumor growth (Fukai et al., 2002). Recent experiments have shown that thrombospondin-1-deficient mice also exhibit increased tumor growth compared to the wild-type mice, as shown here for Col IVα3/tumstatin-deficient mice (Lawler et al., 2001; Rodriguez-Manzaneque et al., 2001). Whether the antiangiogenic function of endostatin is compensated by Col XV or other molecules in the type XVIII collagen-deficient mice remains to be determined (Eklund et al., 2001; Marneros and Olsen, 2001).

In conclusion, this study identifies tumstatin as a physiologically functional protein domain that circulates in the blood. Tumstatin is not a gene product by itself, but is produced when MMP-9 cleaves it from Col IV in BM. The physiological level of tumstatin is dependent on MMP-9, and in its absence, the physiological concentration in the blood declines, potentially facilitating pathological angiogenesis and increased growth of tumors. The tumor suppressor activity of tumstatin seen at supraphysiological concentrations is associated with inhibition of protein synthesis, specifically mediated by mTOR, in the endothelial cells (Maeshima et al., 2002). Based on these results, we propose that endogenous inhibitors like tumstatin function as tumor suppressors, constituting an additional line of defense against tumor growth in the body, similar to tumor suppressor genes such as p53.

Experimental procedures

Cell lines and knockout mice

Lewis lung carcinoma (LLC) cells were grown at 37°C in 5% CO_2 in DMEM with 10% heat-inactivated fetal bovine serum (FBS) and 5 ng/ml plasmocin under sterile tissue culture conditions. Primary mouse lung endothelial cells (MLEC) were isolated from 10- to 14-week-old β3 integrin$^{-/-}$ and wild-type mice. Briefly, MLEC expressing intercellular adhesion molecule-2 (ICAM-2) were enriched using rat anti-mouse ICAM-2 mAb (Pharmingen) conjugated to magnetic beads (Dynabeads M-450, Dynal). MLEC were maintained in 40% Ham's F-12, 40% DME-Low Glucose, 20% FBS supplemented with heparin, endothelial mitogen (Biomedical Technologies, Inc.), glutamine, 100 units/ml of penicillin, and 100 mg/ml of streptomycin.

The Col IVα3 mice were originally described by Miner et al. and Cosgrove et al. (Cosgrove et al., 1996; Miner and Sanes, 1996). The mice were procured from Drs. Sanes, Miner, and Cosgrove and also purchased from the Jackson laboratories. The mice were backcrossed for more than 15 generations into a C57BL/6 background. The β3 integrin$^{-/-}$ mice were originally described by Hodivala-Dilke et al. (Hodivala-Dilke et al., 1999). The MMP-9$^{-/-}$ mice were originally described by Vu et al. (Vu et al., 1998).

Production of recombinant tumstatin and synthetic T7 peptide

Recombinant tumstatin was expressed using 293 human embryonic kidney cells as previously described (Maeshima et al., 2000b). Synthetic TMPFLFCNVNDCNFASRNDYSYWL-T7 peptide (Maeshima et al., 2001b) was synthesized at Tufts University Core Facility and analyzed by mass spectrophotometric analysis and purified by analytical HPLC.

In vivo tumor studies

Age- and sex-matched Col IVα3/tumstatin$^{-/-}$, MMP-9$^{-/-}$, and wild-type (C57BL/6) mice were used for these studies. All mouse studies were reviewed and approved by the animal care and use committee of Beth Israel Deaconess Medical Center. Their backs were shaved and LLC cells were injected subcutaneously on the backs of the mice (1×10^6 cells/mouse). The tumors were measured using Vernier calipers, and the volume was calculated using a standard formula (Width^2 $\times$ Length $\times$ 0.52) (Maeshima et al., 2000b). For Figure 2, 12 tumstatin$^{-/-}$ and 6 wild-type mice were used. Eighteen days after the injection, Col IVα3/tumstatin$^{-/-}$ mice were divided into two groups. Tumstatin protein was intravenously injected into seven Col IVα3/tumstatin$^{-/-}$ mice daily (300 ng) for 8 days in sterile PBS, while only sterile PBS was injected into the other five Col IVα3/tumstatin$^{-/-}$ mice. For Figure 8, eight MMP-9$^{-/-}$ and ten wild-type mice were used. Tumstatin protein was intravenously injected into four MMP-9$^{-/-}$ mice daily (200 ng) for 14 days in sterile PBS when tumors reached 2.0 cm^3 and compared to untreated wild-type mice starting at same tumor size. LLC tumor bearing mice were sacrificed and the tumor and other organs were collected. Some parts of the collected tissues were frozen in OCT compound and also snap-frozen in liquid nitrogen, while other parts were fixed in 10% formalin for histological analysis.

Skin wound healing assay

Excisional (1 cm diameter circular) wounds were made in the epidermis and dermis of five age-and sex-matched Col IVα3/tumstatin$^{-/-}$, five Col IVα3/tumstatin$^{+/-}$, and wild-type mice. Two such skin wounds were created on each mouse. The longest and shortest diameters of the wounds were measured with a Vernier caliper. Areas were calculated, assuming the wounds were approximate ellipses, using the formula [π X (the longest radius) $\times$ (the shortest radius)]. The mice were sacrificed 3 and 10 days after the wound induction. The wounded tissue and the surrounding area were removed, fixed in 10% formalin, or snap-frozen in liquid nitrogen and processed for immunohistochemistry.

Liver regeneration study

Subtotal hepatectomy was performed using Col IVα3/tumstatin$^{-/-,\ +/-}$, and wild-type mice under intraperitoneal ketamine (50 mg/kg) (Parke-Davis) anesthesia with five mice in each group. Seventy percent of the total liver mass, including left and middle lobes, was ligated and removed. Ten days after the operation, BrdU (50 mg/kg) was injected intraperitoneally, 2 hr prior to sacrifice of the mice. The livers were removed and some parts were fixed with 4% paraformaldehyde, and other parts were embedded in OCT compound. BrdU staining was performed using a labeling and detection kit according to the manufacturer's directions (Roche). BrdU-labeling index was calculated as the number of BrdU-labeled hepatocyte nuclei per 200 hepatocyte nuclei, three viewing fields were counted per mouse liver in a blinded fashion. The nuclei were stained with 4′, 6-diamidino-2-phenylindole (DAPI) (Vector Laboratories, App Imaging).

Matrigel plug assay

In vivo Matrigel plug assay was performed as previously described (Maeshima et al., 2000b). Matrigel (BD Biosciences) was mixed with 20 units/ml of heparin (Pierce), 50 ng/ml of vascular endothelial growth factor (R&D), and 0.4 μM tumstatin or 3 μM T7 peptide or 0.5 μM endostatin. The Matrigel mixture was injected subcutaneously into 6 Col IVα3/tumstatin$^{-/-}$, 6 Col IVα3/tumstatin$^{+/+}$, 13 β3 integrin$^{-/-}$, and 10 integrin$^{+/+}$ mice. Six days after the Matrigel mixture injection, mice were sacrificed. The Matrigel plugs were removed and fixed with 4% paraformaldehyde or 10% formalin. They were embedded in paraffin, sectioned, and stained with hematoxylin and eosin (HE) or periodic acid-Schiff (PAS). Other parts were embedded in OCT compound. Sections were examined using 10 different fields by light microscopy, and the numbers of blood vessels at 200$\times$ magnifications were counted and averaged. All sections were coded and observed by an investigator who was blinded for study protocols.

Immunostaining

Immunohistochemical staining was performed as previously described (Hamano et al., 2002). Briefly, 4 μm frozen sections were fixed in cold (−20°C) 100% acetone for 3 min then air dried. They were incubated with various primary antibodies, i.e., rat anti-mouse CD31 (Pharmingen), rabbit anti-von

Willebrand Factor (vWF) (Dako), rat anti-β1 integrin (Pharmingen), and hamster anti-β3 integrin (Pharmingen) antibodies at room temperature for 2 hr. Subsequently, they were washed three times in PBS and incubated with FITC- or tetramethyl rhodamine-conjugated secondary antibodies (Jackson ImmunoResearch Laboratories, Inc.) at room temperature for 1 hr. After four washes with PBS, Vectashield (Vector Laboratories, App Imaging) anti-fade mounting medium was applied and sections were coverslipped and imaged. For controls, sections were directly incubated with secondary antibodies. In each group, the numbers of CD31, vWF, and β1/β3 integrin-positive blood vessels were counted in 10–30 fields at 200× or 400× magnifications in a blinded fashion.

Proliferation assay

Proliferation assay was performed using [^{3}H]-thymidine incorporation as previously described (Kamphaus et al., 2000). Briefly, β3 integrin$^{-/-}$ and wild-type MLEC (16,000 cells/well) in DMEM containing 5% FBS were plated onto 24-well plates. After 24 hr, this medium was replaced with medium containing 20% FBS supplemented with 5 ng/ml of bFGF, 10 ng/ml of VEGF, and either recombinant protein or synthetic peptide at 37°C. One micromolar tumstatin, 4.5 μM T7 peptide, and 4.5 μM endostatin were added for this assay. Control cells were incubated with DMEM containing 20% FBS, 5 ng/ml of bFGF, and 10 ng/ml of VEGF. After 14 hr, all wells received 2 μCi of [^{3}H]-thymidine in DMEM. After 24 hr, the cells were lysed with NaOH, and [^{3}H]-thymidine incorporation was measured using a scintillation counter. All experimental groups represent triplicate samples. At this time point, tumstatin- and endostatin-treated wells were also analyzed for total cell count using the methylene blue staining method (Maeshima et al., 2000b), and there was 15% decrease in the number of cells with respect to control wells (16,000 cells/well). Thus, diminished [^{3}H]-thymidine incorporation is a combination of cell growth arrest and cell death (data not shown). Glomerular BM from bovine kidneys was prepared as previously described (Kalluri et al., 1997b). Ten micrograms of MMP-9 enzyme was added to 1 mg GBM in MMP digestion buffer (50 mM Tris, pH 7.4, 0.2 M NaCl, 10 mM $CaCl_2$, 1 μM $ZnCl_2$, 0.02% Brij) incubated with gentle stirring for 24 hr at 37°C. As a control, 20 mM EDTA was added to the mixture to inactivate MMP enzyme, to assess enzyme-independent solubilization of GBM in the MMP digestion buffer. At the end of 24 hr, the reaction was arrested using 10 mM EDTA. The reaction mix was spun in a high speed centrifuge and the supernatant was analyzed for MMP degradation products. The generation of tumstatin was analyzed by SDS-PAGE and immunoblotting as previously described (Kalluri et al., 1996). Rabbit antibody raised against the C-terminal 36 amino acids of tumstatin (anti-tumstatin) was prepared as previously described (Kalluri et al., 1997b; Reddy et al., 1993). Goat anti-rabbit IgG antibody conjugated with horseradish peroxidase was purchased from Sigma.

ELISA assay of tumstatin

Plasma tumstatin concentration was measured using a modified ELISA assay. A 96-well microplate was coated with 25 μl/well of mouse plasma from wild-type, Col IVα3/tumstatin$^{-/-}$, and MMP-9$^{-/-}$ mice in 0.5 M sodium carbonate (pH 9.7) at room temperature (RT) overnight, washed three times with PBS containing 0.05% Tween 20 (PBST), and blocked with 150 μl/well of PBS containing 1% BSA at 37°C for 1 hr. After washing three times with PBST, rabbit anti-tumstatin antibody was added at 50 μl/well and allowed to react at room temperature for 2 hr. The wells were washed three times with PBST and incubated with 50 μl of goat anti-rabbit IgG antibody conjugated with horseradish peroxidase (Sigma) at room temperature for 1 hr. Then, plates were washed six times with PBST followed by incubation at room temperature for 1 hr with substrate for horseradish peroxidase (HRP). The TMB was used as a substrate (Kirkegaard & Perry Laboratories). For Figure 7, 1 mg of glomerular BM was prepared and subjected to MMP-9 degradation as described (Kalluri et al., 1997a, 1997b). The resulting supernatant after digestion was coated on ELISA plate and detected with anti-tumstatin antibody (Kalluri et al., 1997b).

Measurement of circulating endothelial cells

Five hundred microliters of whole blood was collected from mice in EDTA or heparin using 1 ml microcentrifuge tubes and examined for the number of circulating endothelial cells. After plasma was separated, 300 μl of DMEM supplemented with 10% FBS were added to the tube. Red blood cells were removed with RBC lysis solution (Puregene) and the mixture was placed on 8-chamber slides. After a 6 hr incubation that allowed endothelial cells to attach to the slide, the attached cells were stained with anti-VEGFR2 antibody (Santa Cruz). The VEGFR2-positive cells were counted under the fluorescence microscope in 10 fields at a magnification of 200×.

Litter size and developmental index

For litter size at birth, the average numbers of pups in eight separate litters delivered from Col IVα3/tumstatin$^{-/-}$ and age-matched wild-type mating pairs were counted. For developmental index, the 6 week survival rates of the eight separate litters from both groups were calculated.

Statistical analysis

Statistical differences between two groups were calculated using Student's t test or Welch's t test. Analysis of variance (ANOVA) was used to determine statistical differences among three or more groups. As needed, further analysis was carried out using t test with Bonferroni correction to identify significant differences. A p value <0.05 was considered statistically significant.

Acknowledgments

This study was supported by NIH grants DK 55001 (R.K.), DK 51711 (R.K.), CA72006 (Z.W.), HL66105 (R.H.), HHMI funds (R.H.), and research funds of the Center for Matrix Biology at the BIDMC. Y.H. was supported by Japan Research Foundation for Clinical Pharmacology and is currently by the Stop and Shop Pediatric Brain Tumor Foundation. We would also like to acknowledge the generous financial donations to the Kalluri laboratory from Ann L. and Herbert J. Siegel philanthropic Jewish Communal fund and the Joseph Lubrano Memorial Goldfield Family Charitable trust fund. M.Z. was funded by DFG Grant ZE523/1-1. BIDMC and R.K. are equity holders in Ilex Oncology, a company that has licensed tumstatin patents from the BIDMC. We thank Lori Siniski for the help in preparing this manuscript.

Received: September 10, 2002
Revised: March 26, 2003
Published: June 23, 2003

References

Andrews, K.L., Mudd, J.L., Li, C., and Miner, J.H. (2002). Quantitative trait loci influence renal disease progression in a mouse model of Alport syndrome. Am. J. Pathol. *160*, 721–730.

Bergers, G., Brekken, R., McMahon, G., Vu, T.H., Itoh, T., Tamaki, K., Tanzawa, K., Thorpe, P., Itohara, S., Werb, Z., and Hanahan, D. (2000). Matrix metalloproteinase-9 triggers the angiogenic switch during carcinogenesis. Nat. Cell Biol. *2*, 737–744.

Bramhall, S.R., Hallissey, M.T., Whiting, J., Scholefield, J., Tierney, G., Stuart, R.C., Hawkins, R.E., McCulloch, P., Maughan, T., Brown, P.D., et al. (2002). Marimastat as maintenance therapy for patients with advanced gastric cancer: a randomised trial. Br. J. Cancer *86*, 1864–1870.

Carmeliet, P., and Jain, R.K. (2000). Angiogenesis in cancer and other diseases. Nature *407*, 249–257.

Colorado, P.C., Torre, A., Kamphaus, G., Maeshima, Y., Hopfer, H., Takahashi, K., Volk, R., Zamborsky, E.D., Herman, S., Ericksen, M.B., et al. (2000). Anti-angiogenic cues from vascular basement membrane collagen. Cancer Res. *60*, 2520–2526.

Cosgrove, D., Meehan, D.T., Grunkemeyer, J.A., Kornak, J.M., Sayers, R., Hunter, W.J., and Samuelson, G.C. (1996). Collagen COL4A3 knockout: a mouse model for autosomal Alport syndrome. Genes Dev. *10*, 2981–2992.

Czubayko, F., Liaudet-Coopman, E.D., Aigner, A., Tuveson, A.T., Berchem, G.J., and Wellstein, A. (1997). A secreted FGF-binding protein can serve as the angiogenic switch in human cancer. Nat. Med. *3*, 1137–1140.

Derry, C.J., and Pusey, C.D. (1994). Tissue-specific distribution of the Goodpasture antigen demonstrated by 2-D electrophoresis and western blotting. Nephrol. Dial. Transplant. *9*, 355–361.

Egeblad, M., and Werb, Z. (2002). New functions for the matrix metalloproteinases in cancer progression. Nat. Rev. Cancer *2*, 161–174.

Eklund, L., Piuhola, J., Komulainen, J., Sormunen, R., Ongvarrasopone, C., Fassler, R., Muona, A., Ilves, M., Ruskoaho, H., Takala, T.E., and Pihlajaniemi, T. (2001). Lack of type XV collagen causes a skeletal myopathy and cardiovascular defects in mice. Proc. Natl. Acad. Sci. USA *98*, 1194–1199.

Eliceiri, B.P., Paul, R., Schwartzberg, P.L., Hood, J.D., Leng, J., and Cheresh, D.A. (1999). Selective requirement for Src kinases during VEGF-induced angiogenesis and vascular permeability. Mol. Cell *4*, 915–924.

Ferrara, N. (2000). Vascular endothelial growth factor and the regulation of angiogenesis. Recent Prog. Horm. Res. *55*, 15–35.

Folkman, J. (2001). Angiogenesis-dependent diseases. Semin. Oncol. *28*, 536–542.

Folkman, J., and Kalluri, R. (2003). Tumor angiogenesis. In Cancer Medicine, 6th Editon, J.F. Holland, E. Frei III, R.C. Bast, Jr., D.W. Kufe, R.E. Pollock, R.R. Weichselbaum, eds. (Ontario, Canada: PC Decker Inc.), in press.

Frojdman, K., Pelliniemi, L.J., and Virtanen, I. (1998). Differential distribution of type IV collagen chains in the developing rat testis and ovary. Differentiation *63*, 125–130.

Fukai, N., Eklund, L., Marneros, A.G., Oh, S.P., Keene, D.R., Tamarkin, L., Niemela, M., Ilves, M., Li, E., Pihlajaniemi, T., and Olsen, B.R. (2002). Lack of collagen XVIII/endostatin results in eye abnormalities. EMBO J. *21*, 1535–1544.

Gabrielli, A., Marchegiani, G., Rupoli, S., Ansuini, G., Brocks, D.G., Danieli, G., and Timpl, R. (1988). Assessment of disease activity in essential cryoglobulinemia by serum levels of a basement membrane antigen, laminin. Arthritis Rheum. *31*, 1558–1562.

Gunwar, S., Ballester, F., Kalluri, R., Timoneda, J., Chonko, A.M., Edwards, S.J., Noelken, M.E., and Hudson, B.G. (1991). Glomerular basement membrane. Identification of dimeric subunits of the noncollagenous domain (hexamer) of collagen IV and the Goodpasture antigen. J. Biol. Chem. *266*, 15318–15324.

Hamano, Y., Grunkemeyer, J.A., Sudhakar, A., Zeisberg, M., Cosgrove, D., Morello, R., Lee, B., Sugimoto, H., and Kalluri, R. (2002). Determinants of vascular permeability in the kidney glomerulus. J. Biol. Chem. *277*, 31154–31162.

Hanahan, D., and Weinberg, R.A. (2000). The hallmarks of cancer. Cell *100*, 57–70.

Hawighorst, T., Velasco, P., Streit, M., Hong, Y.K., Kyriakides, T.R., Brown, L.F., Bornstein, P., and Detmar, M. (2001). Thrombospondin-2 plays a protective role in multistep carcinogenesis: a novel host anti-tumor defense mechanism. EMBO J. *20*, 2631–2640.

Heissig, B., Hattori, K., Dias, S., Friedrich, M., Ferris, B., Hackett, N.R., Crystal, R.G., Besmer, P., Lyden, D., Moore, M.A., et al. (2002). Recruitment of stem and progenitor cells from the bone marrow niche requires MMP-9 mediated release of kit-ligand. Cell *109*, 625–637.

Hodivala-Dilke, K.M., McHugh, K.P., Tsakiris, D.A., Rayburn, H., Crowley, D., Ullman-Cullere, M., Ross, F.P., Coller, B.S., Teitelbaum, S., and Hynes, R.O. (1999). β3-integrin-deficient mice are a model for Glanzmann thrombasthenia showing placental defects and reduced survival. J. Clin. Invest. *103*, 229–238.

Hogemann, B., Voss, B., Pott, G., Rauterberg, J., and Gerlach, U. (1984). 7S collagen: a method for the measurement of serum concentrations in man. Clin. Chim. Acta. *144*, 1–10.

Hudson, B.G., Reeders, S.T., and Tryggvason, K. (1993). Type IV collagen: structure, gene organization, and role in human diseases. Molecular basis of Goodpasture and Alport syndromes and diffuse leiomyomatosis. J. Biol. Chem. *268*, 26033–26036.

Hynes, R.O. (2002a). A reevaluation of integrins as regulators of angiogenesis. Nat. Med. *8*, 918–921.

Hynes, R.O., Lively, J.C., McCarty, J.H., Taverna, D., Xiao, Q., and Hodivala-Dilke, K. (2002b). Diverse roles of integrins and their ligands in angiogenesis. Cold Spring Harb. Symp. Quant. Biol. *67*, 143–153.

Kahsai, T.Z., Enders, G.C., Gunwar, S., Brunmark, C., Wieslander, J., Kalluri, R., Zhou, J., Noelken, M.E., and Hudson, B.G. (1997). Seminiferous tubule basement membrane. Composition and organization of type IV collagen chains, and the linkage of α3(IV) and α5(IV) chains. J. Biol. Chem. *272*, 17023–17032.

Kalluri, R. (2002). Discovery of type IV collagen non collagenous domains as endogenous inhibitors of angiogenesis and tumor growth and novel integrin ligands. Cold Spring Harb. Symp. Quant. Biol. *67*, 255–266.

Kalluri, R., and Cosgrove, D. (2000). Assembly of type IV collagen. Insights from α3(IV) collagen-deficient mice. J. Biol. Chem. *275*, 12719–12724.

Kalluri, R., Sun, M.J., Hudson, B.G., and Neilson, E.G. (1996). The Goodpasture autoantigen. Structural delineation of two immunologically privileged epitopes on α3(IV) chain of type IV collagen. J. Biol. Chem. *271*, 9062–9068.

Kalluri, R., Danoff, T.M., Okada, H., and Neilson, E.G. (1997a). Susceptibility to anti-glomerular basement membrane disease and Goodpasture syndrome is linked to MHC class II genes and the emergence of T cell-mediated immunity in mice. J. Clin. Invest. *100*, 2263–2275.

Kalluri, R., Shield, C.F., Todd, P., Hudson, B.G., and Neilson, E.G. (1997b). Isoform switching of type IV collagen is developmentally arrested in X-linked Alport syndrome leading to increased susceptibility of renal basement membranes to endoproteolysis. J. Clin. Invest. *99*, 2470–2478.

Kamphaus, G.D., Colorado, P.C., Panka, D.J., Hopfer, H., Ramchandran, R., Torre, A., Maeshima, Y., Mier, J.W., Sukhatme, V.P., and Kalluri, R. (2000). Canstatin, a novel matrix-derived inhibitor of angiogenesis and tumor growth. J. Biol. Chem. *275*, 1209–1215.

Kashtan, C.E. (1998). Alport syndrome and thin glomerular basement membrane disease. J. Am. Soc. Nephrol. *9*, 1736–1750.

Kuhn, K. (1995). Basement membrane (type IV) collagen. Matrix Biol. *14*, 439–445.

Lawler, J., Miao, W.M., Duquette, M., Bouck, N., Bronson, R.T., and Hynes, R.O. (2001). Thrombospondin-1 gene expression affects survival and tumor spectrum of p53-deficient mice. Am. J. Pathol. *159*, 1949–1956.

Lyden, D., Hattori, K., Dias, S., Costa, C., Blaikie, P., Butros, L., Chadburn, A., Heissig, B., Marks, W., Witte, L., et al. (2001). Impaired recruitment of bone-marrow-derived endothelial and hematopoietic precursor cells blocks tumor angiogenesis and growth. Nat. Med. *7*, 1194–1201.

Madri, J.A. (1997). Extracellular matrix modulation of vascular cell behaviour. Transpl. Immunol. *5*, 179–183.

Madri, J.A., and Pratt, B.M. (1986). Endothelial cell-matrix interactions: in vitro models of angiogenesis. J. Histochem. Cytochem. *34*, 85–91.

Maeshima, Y., Colorado, P.C., and Kalluri, R. (2000a). Two RGD-independent αvβ3 integrin binding sites on tumstatin regulate distinct anti-tumor properties. J. Biol. Chem. *275*, 23745–23750.

Maeshima, Y., Colorado, P.C., Torre, A., Holthaus, K.A., Grunkemeyer, J.A., Ericksen, M.D., Hopfer, H., Xiao, Y., Stillman, I.E., and Kalluri, R. (2000b). Distinct anti-tumor properties of a type IV collagen domain derived from basement membrane. J. Biol. Chem. *275*, 21340–21348.

Maeshima, Y., Manfredi, M., Reimer, C., Holthaus, K.A., Hopfer, H., Chandamuri, B.R., Kharbanda, S., and Kalluri, R. (2001a). Identification of the anti-angiogenic site within vascular basement membrane derived tumstatin. J. Biol. Chem. *276*, 15240–15248.

Maeshima, Y., Yerramalla, U.L., Dhanabal, M., Holthaus, K.A., Barbashov, S., Kharbanda, S., Reimer, C., Manfredi, M., Dickerson, W.M., and Kalluri, R. (2001b). Extracellular matrix-derived peptide binds to αvβ3 integrin and inhibits angiogenesis. J. Biol. Chem. *276*, 31959–31968.

Maeshima, Y., Sudhakar, A., Lively, J.C., Ueki, K., Kharbanda, S., Kahn, C.R., Sonenberg, N., Hynes, R.O., and Kalluri, R. (2002). Tumstatin, an endothelial cell-specific inhibitor of protein synthesis. Science *295*, 140–143.

Maragoudakis, M.E., Missirlis, E., Karakiulakis, G.D., Sarmonica, M., Bastakis, M., and Tsopanoglou, N. (1993). Basement membrane biosynthesis as a target for developing inhibitors of angiogenesis with anti-tumor properties. Kidney Int. *43*, 147–150.

Maragoudakis, M.E., Haralabopoulos, G.C., Tsopanoglou, N.E., and Pipili-

Synetos, E. (1995). Validation of collagenous protein synthesis as an index for angiogenesis with the use of morphological methods. Microvasc. Res. *50*, 215–222.

Marneros, A.G., and Olsen, B.R. (2001). The role of collagen-derived proteolytic fragments in angiogenesis. Matrix Biol. *20*, 337–345.

McCawley, L.J., and Matrisian, L.M. (2001). Matrix metalloproteinases: they're not just for matrix anymore! Curr. Opin. Cell Biol. *13*, 534–540.

Miner, J.H., and Sanes, J.R. (1996). Molecular and functional defects in kidneys of mice lacking collagen α3(IV): implications for Alport syndrome. J. Cell Biol. *135*, 1403–1413.

Monestiroli, S., Mancuso, P., Burlini, A., Pruneri, G., Dell'Agnola, C., Gobbi, A., Martinelli, G., and Bertolini, F. (2001). Kinetics and viability of circulating endothelial cells as surrogate angiogenesis marker in an animal model of human lymphoma. Cancer Res. *61*, 4341–4344.

O'Reilly, M.S., Holmgren, L., Shing, Y., Chen, C., Rosenthal, R.A., Moses, M., Lane, W.S., Cao, Y., Sage, E.H., and Folkman, J. (1994). Angiostatin: a novel angiogenesis inhibitor that mediates the suppression of metastases by a Lewis lung carcinoma. Cell *79*, 315–328.

O'Reilly, M.S., Boehm, T., Shing, Y., Fukai, N., Vasios, G., Lane, W.S., Flynn, E., Birkhead, J.R., Olsen, B.R., and Folkman, J. (1997). Endostatin: an endogenous inhibitor of angiogenesis and tumor growth. Cell *88*, 277–285.

Ortega, N., and Werb, Z. (2002). New functional roles for non-collagenous domains of basement membrane collagens. J. Cell Sci. *115*, 4201–4214.

Padera, T.P., Kadambi, A., di Tomaso, E., Carreira, C.M., Brown, E.B., Boucher, Y., Choi, N.C., Mathisen, D., Wain, J., Mark, E.J., et al. (2002). Lymphatic metastasis in the absence of functional intratumor lymphatics. Science *296*, 1883–1886.

Paulsson, M. (1992). Basement membrane proteins: structure, assembly, and cellular interactions. Crit. Rev. Biochem. Mol. Biol. *27*, 93–127.

Petitclerc, E., Boutaud, A., Prestayko, A., Xu, J., Sado, Y., Ninomiya, Y., Sarras, M.P., Jr., Hudson, B.G., and Brooks, P.C. (2000). New functions for Non-collagenous domains of human collagen type IV. Novel integrin ligands inhibiting angiogenesis and tumor growth in vivo. J. Biol. Chem. *275*, 8051–8061.

Polette, M., Thiblet, J., Ploton, D., Buisson, A.C., Monboisse, J.C., Tournier, J.M., and Birembaut, P. (1997). Distribution of α1(IV) and α3(IV) chains of type IV collagen in lung tumours. J. Pathol. *182*, 185–191.

Pozzi, A., Moberg, P.E., Miles, L.A., Wagner, S., Soloway, P., and Gardner, H.A. (2000). Elevated matrix metalloprotease and angiostatin levels in integrin α1 knockout mice cause reduced tumor vascularization. Proc. Natl. Acad. Sci. USA *97*, 2202–2207.

Pozzi, A., LeVine, W.F., and Gardner, H.A. (2002). Low plasma levels of matrix metalloproteinase 9 permit increased tumor angiogenesis. Oncogene *21*, 272–281.

Prockop, D.J., and Kivirikko, K.I. (1995). Collagens: molecular biology, diseases, and potentials for therapy. Annu. Rev. Biochem. *64*, 403–434.

Reddy, G.K., Gunwar, S., Kalluri, R., Hudson, B.G., and Noelken, M.E. (1993). Structure and composition of type IV collagen of bovine aorta. Biochim. Biophys. Acta *1157*, 241–251.

Reynolds, L.E., Wyder, L., Lively, J.C., Taverna, D., Robinson, S.D., Huang, X., Sheppard, D., Hynes, R.O., and Hodivala-Dilke, K.M. (2002). Enhanced pathological angiogenesis in mice lacking β3 integrin or β3 and β5 integrins. Nat. Med. *8*, 27–34.

Rodriguez-Manzaneque, J.C., Lane, T.F., Ortega, M.A., Hynes, R.O., Lawler, J., and Iruela-Arispe, M.L. (2001). Thrombospondin-1 suppresses spontaneous tumor growth and inhibits activation of matrix metalloproteinase-9 and mobilization of vascular endothelial growth factor. Proc. Natl. Acad. Sci. USA *98*, 12485–12490.

Stacker, S.A., Achen, M.G., Jussila, L., Baldwin, M.E., and Alitalo, K. (2002). Metastasis: Lymphangiogenesis and cancer metastasis. Nat. Rev. Cancer *2*, 573–583.

Standker, L., Schrader, M., Kanse, S.M., Jurgens, M., Forssmann, W.G., and Preissner, K.T. (1997). Isolation and characterization of the circulating form of human endostatin. FEBS Lett. *420*, 129–133.

Thyboll, J., Kortesmaa, J., Cao, R., Soininen, R., Wang, L., Iivanainen, A., Sorokin, L., Risling, M., Cao, Y., and Tryggvason, K. (2002). Deletion of the laminin α4 chain leads to impaired microvessel maturation. Mol. Cell. Biol. *22*, 1194–1202.

Timpl, R. (1996). Macromolecular organization of basement membranes. Curr. Opin. Cell Biol. *8*, 618–624.

Tsilibary, E.C., Reger, L.A., Vogel, A.M., Koliakos, G.G., Anderson, S.S., Charonis, A.S., Alegre, J.N., and Furcht, L.T. (1990). Identification of a multifunctional, cell-binding peptide sequence from the α1(NC1) of type IV collagen. J. Cell Biol. *111*, 1583–1591.

Volpert, O.V., Zaichuk, T., Zhou, W., Reiher, F., Ferguson, T.A., Stuart, P.M., Amin, M., and Bouck, N.P. (2002). Inducer-stimulated Fas targets activated endothelium for destruction by anti-angiogenic thrombospondin-1 and pigment epithelium-derived factor. Nat. Med. *8*, 349–357.

Vu, T.H., Shipley, J.M., Bergers, G., Berger, J.E., Helms, J.A., Hanahan, D., Shapiro, S.D., Senior, R.M., and Werb, Z. (1998). MMP-9/gelatinase B is a key regulator of growth plate angiogenesis and apoptosis of hypertrophic chondrocytes. Cell *93*, 411–422.

Yudoh, K., Matsui, H., Kanamori, M., Ohmori, K., Tsuji, H., and Tatezaki, S. (1994). Serum levels of laminin, type IV collagen and type III procollagen peptide as markers for detection of metastasis. Jpn. J. Cancer Res. *85*, 1263–1269.

Yurchenco, P.D., and O'Rear, J.J. (1994). Basal lamina assembly. Curr. Opin. Cell Biol. *6*, 674–681.

Zeisberg, M., Bonner, G., Maeshima, Y., Colorado, P., Muller, G.A., Strutz, F., and Kalluri, R. (2001). Renal fibrosis: collagen composition and assembly regulates epithelial-mesenchymal transdifferentiation. Am. J. Pathol. *159*, 1313–1321.

Zhang, X., Hudson, B.G., and Sarras, M.P., Jr. (1994). Hydra cell aggregate development is blocked by selective fragments of fibronectin and type IV collagen. Dev. Biol. *164*, 10–23.